Is the new CDF M_W measurement consistent with the two-Higgs doublet model?

H. Abouabid [a], A. Arhrib [a], R. Benbrik [b], M. Krab [c,*], M. Ouchemhou [b]

[a] *Abdelmalek Essaadi University, Faculty of Sciences and Techniques, Tangier, Morocco*
[b] *Laboratory of Fundamental and Applied Physics, Faculté Polydisciplinaire de Safi, Sidi Bouzid, BP 4162, Safi, Morocco*
[c] *Research Laboratory in Physics and Engineering Sciences, Modern and Applied Physics Team, Polydisciplinary Faculty, Beni Mellal, 23000, Morocco*

Abstract

Motivated by the recent CDF measurement of the W boson mass, which clearly demonstrates a significant deviation from the prediction of the Standard Model (SM). In the present paper, we study the Two-Higgs Doublet Model (2HDM) contribution to M_W and its phenomenological implications in the case where the heavy CP-even H is identified as the observed Higgs boson with a mass of 125 GeV. Taking into account theoretical and current experimental constraints, as well as the new CDF measurement, we demonstrate that the 2HDM parameter space can provide a significant correction which predicts the W mass close to the new CDF M_W measurement. It is found that $M_{H^\pm} = M_A$ is excluded, and the splitting of the charged Higgs boson with all other states is positive. We also discuss the effects on the effective mixing angle $\sin^2 \theta_{\text{eff}}$ as well as the phenomenological implications on the charged Higgs and CP-odd Higgs boson decays in 2HDM type-I and type-X.

---

* Corresponding author.
 E-mail addresses: hamza.abouabid@gmail.com (H. Abouabid), aarhrib@gmail.com (A. Arhrib), r.benbrik@uca.ma (R. Benbrik), mohamed.krab@usms.ac.ma (M. Krab), ouchemhou2@gmail.com (M. Ouchemhou).

1. Introduction

Electro-Weak Precision Observables (EWPOs) such as W boson mass, the effective mixing angle $\sin^2 \theta_{\text{eff}}$ and the Z boson width and so on, can be used to test the validity of the Standard Model (SM) and to reveal the presence of new physics.

After a decade of work, using the data set collected at 8.8 fb^{-1} of luminosity and 1.96 TeV center-of-mass energy at the Tevatron, the CDF collaboration discovered that the W boson has a mass of [1,2]:

$$M_W^{\text{CDF}} = 80.4435 \pm 0.0094 \text{ GeV}. \tag{1}$$

The precision with which this measurement was carried out, 0.01%, exceeds all previous measurements combined. In addition, the new value agrees with many previous W mass measurements, but there are also some disagreements [3]. Therefore, future measurements will be needed to further shed light on the outcome. The above measurement should be compared to the SM prediction [3,4],

$$M_W^{\text{SM}} = 80.357 \pm 0.006 \text{ GeV}. \tag{2}$$

Note that the above value is based on complex SM radiative corrections that closely relate the mass of the W to the measurements of the masses of the top quark and the Higgs boson. It is clear that M_W^{CDF} presents a deviation from M_W^{SM} with a significance of 7σ.

In the past, during the LEP era, it was well-known that the global fit of the SM to LEP and SLC data has been used to predict the existence of heavy top quark and relatively light Higgs boson well before their discovery at Tevatron and LHC respectively. Although the CDF measurement needs to be confirmed shortly, it is quite likely that the difference between the experimental value and the expected SM value is due to a non-decoupled new particle or a new interaction. If it is the case, there is a chance that these new phenomena will show up in future experiments.

Moreover, it is well known that the discrepancy of M_W^{CDF} from the SM prediction can be parameterized in terms of the oblique parameters, S, T and U [5,6] which are a combination of gauge bosons self-energies. All new particles, if not too heavy and interact with the photon, W and Z bosons, will contribute to S, T and U and can, therefore, reduce the tension between M_W^{CDF} and M_W^{SM}.

In the present paper, we will discuss the implications of the new CDF measurement on the Two-Higgs Doublet Model (2HDM), which predicts in its spectrum two CP-even, h and H (with $M_h < M_H$), one CP-odd A and a pair of charged Higgs $H^\pm$. Recently, there have been several studies addressing a similar issue within the 2HDM [8–21], triplet extension [22–25] and also other SM extensions [26–51]. In this study, we identify the observed SM Higgs with H whose properties are consistent with the LHC measurements and assume that the second CP-even Higgs is lighter than 125 GeV. We will explain how the 2HDM can solve the tension between CDF measurement and the SM prediction and give some phenomenological implications on charged Higgs and CP-odd Higgs boson decays both in 2HDM type-I and type-X.

The paper is organized as follows. In the second section, we briefly introduce the setup of the 2HDM and give the S, T and U formalism for the computation of M_W^{2HDM} and $\sin^2 \theta_{\text{eff}}^{\text{2HDM}}$. In the third section, we present the details of our scan as well as the theoretical and experimental constraints used to constrain the parameter space. We then present our main result and explain how the 2HDM spectrum can predict the W mass that is close to the new CDF measurement. In addition, we give phenomenological implications for the charged Higgs and CP-odd boson decays within the allowed parameter space. We conclude in section four.

2. M_W in the 2HDM

The 2HDM framework is one of the simplest extensions of the SM Higgs sector. It contains two Higgs doublet fields, ϕ_1 and ϕ_2, that can interact with fermions and gauge bosons to generate their masses.

The CP-conserving 2HDM potential which is invariant under $SU_L(2) \times U_Y(1)$ can be written as

$$
\begin{aligned}
V(\phi_1, \phi_2) = &\, m_{11}^2(\phi_1^\dagger \phi_1) + m_{22}^2(\phi_2^\dagger \phi_2) - [m_{12}^2(\phi_1^\dagger \phi_2) + \text{h.c.}] \\
&+ \frac{1}{2}\lambda_1(\phi_1^\dagger \phi_1)^2 + \frac{1}{2}\lambda_2(\phi_2^\dagger \phi_2)^2 + \lambda_3(\phi_1^\dagger \phi_1)(\phi_2^\dagger \phi_2) \\
&+ \lambda_4(\phi_1^\dagger \phi_2)(\phi_2^\dagger \phi_1) + \frac{1}{2}\left[\lambda_5(\phi_1^\dagger \phi_2)^2 + \text{h.c.}\right],
\end{aligned}
\tag{1}
$$

where $\lambda_{1,2,3,4,5}$ as well as m_{11}^2 and m_{22}^2 are chosen to be real. If both Higgs fields interact with all SM fermions, like in the SM, we end up with Flavour Changing Neutral Currents (FCNCs) at the tree level in the Yukawa sector. In order to avoid such FCNCs, a discrete Z_2 symmetry is introduced to prevent large tree-level FCNCs [52,53]. Such a discrete symmetry is imposed both on the Yukawa sector as well as the scalar potential where we allow for a soft violation of Z_2 by $m_{12}^2(\phi_1^\dagger \phi_2)$ term. Moreover, under the Z_2 symmetry, there are four possible types of Yukawa sector: type-I, type-II, type-X (or lepton-specific) and type-Y (or flipped). Here, in this work, we shall focus on type-I and -X models. In the 2HDM type-I, ϕ_2 doublet couples to all the SM fermions exactly like in the SM while in the 2HDM type-X all the quarks couple to ϕ_2 and the charged leptons couple to ϕ_1.

Using the two minimization conditions, m_{11}^2 and m_{22}^2 can be expressed as functions of other parameters. The combination of v_1 and v_2 is fixed from the electroweak scale: $v_1^2 + v_2^2 = v^2 \simeq$ (246 GeV)^2. We thus end up with seven independent parameters, namely $\lambda_{1,2,3,4,5}$, m_{12}^2 and $\tan\beta$. Alternatively, the set M_h, M_H, M_A, $M_{H^\pm}$, $\sin(\beta-\alpha)$, $\tan\beta$ and m_{12}^2 can be chosen instead. α is the mixing angle between the two CP-even scalars h and H, while β is the ratio of the vacuum expectation values, $\tan\beta = v_2/v_1$.

The 2HDM contribution to the EWPOs can be described by the oblique parameters formalism, which is a good one to parameterize the effects of new physics on EW observables. A convenient parametrization of such formalism is given by the well-known parameters S, T and U [5,6]. In the 2HDM, the ρ parameter, which is the ratio of neutral and charged current at small momentum transfers, is related to the oblique parameter T. Such a contribution is controlled by the so-called custodial symmetry to preserve the tree-level value of ρ parameter, $\rho = M_W^2/(c_W^2 M_Z^2) \approx 1$, which is in good agreement with experiments. As discussed in the literature, in the SM, the custodial symmetry is broken both by the hypercharge and by the different sizes of the Yukawas, while in the 2HDM, the custodial symmetry can be restored in the scalar sector so long the Higgs states are degenerate in mass.

In general, the contribution of 2HDM to W boson mass can be expressed in terms of the parameters S, T and U [6,7], i.e.

$$
\Delta M_W^2 = \frac{\alpha_0 c_W^2 M_Z^2}{c_W^2 - s_W^2}\left[-\frac{1}{2}S + c_W^2 T + \frac{c_W^2 - s_W^2}{4s_W^2}U\right],
\tag{2}
$$

where $\Delta M_W^2 = (M_W^{2\text{HDM}})^2 - (M_W^{\text{SM}})^2$, M_Z is the Z boson mass, $c_W = M_W^{\text{SM}}/M_Z$ and s_W are cosine and sine of the weak mixing angle ($s_W^2 = 1 - c_W^2$), respectively, and α_0 is the fine structure constant at the Thomson limit.

We also study the effects of the 2HDM spectrum on the effective weak mixing angle, $\sin^2\theta_{\text{eff}}$. This is computed using the following relation [6]:

$$\Delta \sin^2\theta_{\text{eff}} = \frac{\alpha_0}{c_W^2 - s_W^2}\left[\frac{1}{4}S - s_W^2 c_W^2 T\right].\tag{3}$$

Where $\Delta \sin^2\theta_{\text{eff}}$ is the difference between the 2HDM and the SM value. Note that in both Eq. (2) and Eq. (3), the dominant correction to the W boson mass and $\sin^2\theta_{\text{eff}}$ comes from $T(\equiv \delta\rho/\alpha_0)$ parameter, which is sensitive to the mass splitting of 2HDM scalar particles. The size of the T parameter could be viewed as the amount of violation of the Custodial symmetry by the 2HDM spectrum. The SM values used in our calculation are given in Ref. [3]. Analytic expressions for S, T and U parameters in the 2HDM are given in [54].

3. Results and discussions

To study the implication of the new CDF measurement on the 2HDM, we consider the 2HDM type-I and type-X[1] and perform a systematic scan over their parameter space. The scan is done using the public program `2HDMC-1.8.0` [54]. We assume that the CP-even Higgs boson H is the observed SM-like Higgs with $M_H = 125.09$ GeV [55], whose properties are consistent with the LHC measurements. In addition, we suppose that the light CP-even h is lighter than 125 GeV and check that it is consistent with the previous negative LEP and LHC searches. We randomly sample the remaining model parameters within the following ranges:

$$M_h \in [15, 120]\text{ GeV}, \quad M_A \in [15, 700]\text{ GeV},\tag{4}$$
$$M_{H^\pm} \in [80, 700]\text{ GeV}, \quad \sin(\beta - \alpha) \in [-0.5, 0.5],$$
$$\tan\beta \in [2, 25], \quad m_{12}^2 \in [0, M_h^2 \sin\beta\cos\beta]\text{ GeV}^2.$$

During the scan, the following theoretical and experimental constraints are fulfilled:

- Unitarity, perturbativity and vacuum stability are imposed via `2HDMC`.
- Exclusion bounds at 95% Confidence Level (CL) from additional Higgs bosons are enforced via `HiggsBounds-5.9.0` [56].
- Compliance with SM-like Higgs state measurements is enforced via `HiggsSignals-2.6.0` [57].
- Constraints from flavor physics are enforced using the result given in Ref. [58]. Related observables are calculated using the program `SuperIso v4.1` [59].
- Compatibility with the Z width measurement from LEP, $\Gamma_Z = 2.4952 \pm 0.0023$ GeV [60]. The partial width $\Gamma(Z \to hA)$, when is kinematically open, was chosen to satisfy the 2σ experimental uncertainty of the measurement.

---

[1] The 2HDM contribution to ΔM_W is expected to be the same in all Yukawa types at the one-loop level. The main difference comes from LHC constraints on Higgs physics.

We have considered m_{12}^2 to lie in the 0 and $M_h^2 \sin\beta \cos\beta$ range since it has more surviving parameter points compared to a general scan, for instance, from 0 to 10^6. Nevertheless, we expect that our results would not change in case we consider a general scan.

Once we get the allowed parameter space that satisfies all the above theoretical and experimental constraints, we then apply the following $\chi^2_{M_W^{\text{CDF}}}$ test where we take only points that are within 2σ of the new CDF measurement:

$$\chi^2_{M_W^{\text{CDF}}} = \frac{(M_W^{\text{2HDM}} - M_W^{\text{CDF}})^2}{(\Delta M_W^{\text{CDF}})^2}, \tag{5}$$

where $\Delta M_W^{\text{CDF}} = 0.0094$ GeV is the uncertainty of the new CDF measurement (see Eq. (1)). For 2HDM type-X, the Lepton Flavor Universality (LFU) requirements constrain large $\tan\beta$ and light pseudo-scalar mass [61]. Since we are not interested in explaining muon $g-2$, which requires large coupling of pseudo-scalar Higgs boson to the leptons (large $\tan\beta$) and light M_A, we consider $\tan\beta < 25$ and thus constraints from LFU might not affect our results. However, an explanation of the CDF M_W measurement and muon $g-2$ anomalies in the 2HDM type-X can be found in Ref. [62].

In Fig. 1 (left panel), we present the 2HDM prediction for the W boson mass in the allowed parameter space as a function of T, where the color map shows the possible size of S. The light orange band shows the new CDF result for M_W within the 1σ uncertainty. We also depict via light yellow region the SM prediction at the 1σ level. As expected from Eq. (2), the dominant contribution arises from the T parameter, which is almost a linear relation. M_W receives a negative correction from S as indicated by the color code. The dependence of M_W on U is found to be negligible compared to T. It is obvious from Eq. (2) that negative range of the S parameter and positive values of T and U are indeed favored by the new CDF measurement for M_W. Therefore, close to the alignment limit $\cos(\beta - \alpha) \approx 1$, the degenerate case $M_A = M_{H^\pm}$ of the 2HDM is excluded by this new measurement because it would make T vanish. Note that based on the values of S and T obtained by the recent results of Gfitter analysis [8], we further apply the χ^2_{ST} test, which confirms our findings (see Appendix B). Our results are confirmed by further recent works [13,17]. In addition to these works, in Ref. [63], the W-mass shift has been computed within the 2HDM in both normal and inverted hierarchies, predicting corrections of order $20 - 40$ MeV. In the case of inverted hierarchy ($\alpha = \beta$), we found that the W boson mass can be shifted by order 20 MeV using the formula in Eq. (2).

Another important precision observable is the effective weak mixing angle, $\sin^2\theta_{\text{eff}}$. The 2HDM prediction for M_W and $\sin^2\theta_{\text{eff}}$ is depicted in the right panel of Fig. 1. The light violet band indicates the SLD $\sin^2\theta_{\text{eff}}$ measurement within the 1σ uncertainty [60]. We also show via the dark violet region the world average value for $\sin^2\theta_{\text{eff}}$ at the 1σ level (for comparison) [60]. It can be clearly seen that M_W within the 2σ level is in good compliance with the SLD measurement, which is not the case for the world average value. Note that the input for s_W^2 is the on-shell relation, i.e. $s_W^2 = 1 - M_W^2/M_Z^2$. We further test other schemes as input for s_W^2, and the results remain intact, i.e. M_W values in light of the CDF M_W measurement are still in good agreement with the SLD measurement. Similar results were obtained in Refs. [12,14].

As a first implication, we investigate the impact of the new CDF measurement on the spectrum of 2HDM in the inverted hierarchy. In 2HDM in the normal hierarchy, $M_h = 125$ GeV and $M_H > M_h$, it was shown recently that both $M_{H^\pm} > M_H, M_A$ and $M_{H^\pm} < M_H, M_A$ are favored by the new CDF measurement for M_W, whereas the case where $M_{H^\pm} \sim M_H \sim M_A$ is disfavored in the alignment limit of the 2HDM [12,17].
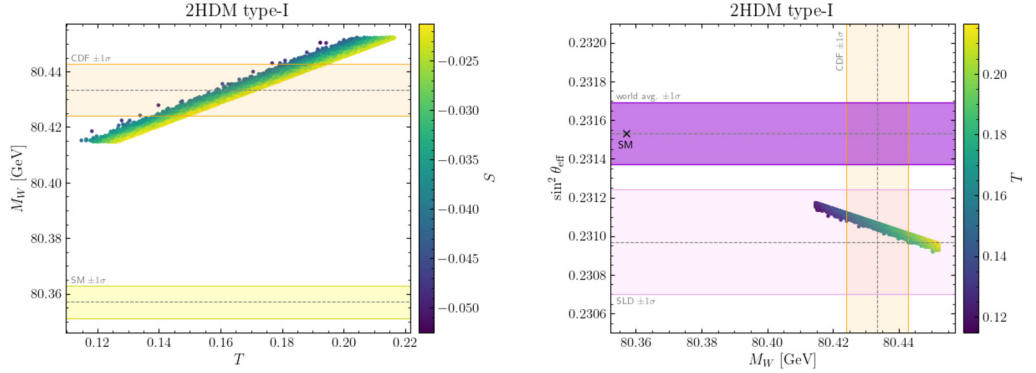
Fig. 1. Left: The 2HDM prediction for the W boson mass as a function of T, with the color bar showing the size of S. The light orange band indicates the new CDF measurement and the associated 1σ uncertainty. The SM prediction for M_W is given by the light yellow region within $\pm 1\sigma$. Right: The 2HDM prediction for M_W and $\sin^2 \theta_{\rm eff}$, with the color bar refers to T. The light orange band indicates the new CDF measurement and the associated 1σ uncertainty. The light and dark violet regions represent the SLD and world average results for $\sin^2 \theta_{\rm eff}$ within the 1σ level, respectively. The SM prediction for M_W and $\sin^2 \theta_{\rm eff}$ is given by the black cross.

In the inverted hierarchy, we illustrate in Fig. 2 the splitting $M_{H^\pm} - M_A$ as a function of $M_{H^\pm} - M_h$ (left panel) and $M_{H^\pm} - M_H$ (right panel), with ΔM_W color coded and represented in the vertical panel. The CDF M_W measurement forces $M_{H^\pm}$ to be always heavier than the neutral Higgses. The case $M_{H^\pm} < M_h, M_H, M_A$ is disfavored since it produces a negative or small T and can not account for the new CDF measurement. Another outcome of the scan is that the new CDF M_W measurement pushes the charged Higgs mass to be larger than 155 GeV[2]. For completeness, we show in Fig. A.1 of Appendix A the full scan for M_W as a function of S (left plot) and as a function of T (right plot). The green points are the one that reproduces the new CDF measurement, while the blue points do not give the correct M_W mass. Similarly, we illustrate in Fig. A.2 of Appendix A the full scan for $M_{H^\pm} - M_A$ as a function of $M_{H^\pm} - M_h$ (left plot) and $M_{H^\pm} - M_H$ (right plot). Only the green band reproduces the new CDF measurement for M_W. It is clear from the plots that this measurement pushes the charged Higgs mass to be larger than 155 GeV.

The results shown in the previous plots are for 2HDM type-I. For 2HDM type-X, we obtain similar plots. The reason is that $\Delta M_W^{\rm 2HDM}$ depends only on S, T and U, which are a combination of gauge bosons self-energies that contains the contribution of the additional Higgs bosons. The gauge boson coupling to the Higgs boson does not depend on the Yukawa type. The only difference between type-I and type-X would come from the LHC constraints. Such constraints depend on the production cross section of the Higgs and its branching ratios, which are sensitive to the Yukawa type. Note also that the combination of EWPOs and the theoretical constraints set a limit on the masses of the heavy states $H^\pm$ and A to be less than about 600 GeV. However, since, in type-II and type-Y, the $B \to X_s \gamma$ observable pushes the mass of the charged Higgs boson to be around 800 GeV, these models are entirely excluded.

We move now to discuss phenomenological consequences on the charged Higgs, CP-odd Higgs and the light CP-even Higgs decays in 2HDM type-I and type-X. In the upper-left panel of Fig. 3, we depict the branching ratios of $H^\pm$ as a function of $M_{H^\pm}$. As one can see, the dominant

---

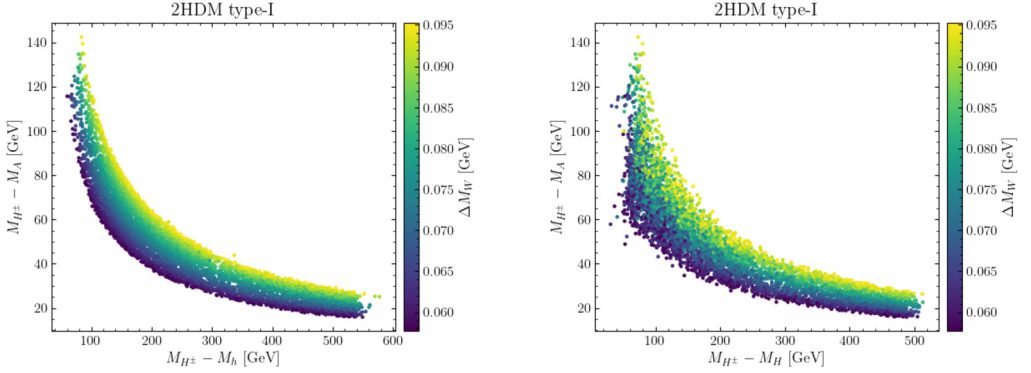[2] We should note that this upper limit is not absolute and that further points may lie below this limit.

Fig. 2. Points from the scan in the $(M_{H^\pm} - M_h, M_{H^\pm} - M_A)$ plane (left) and $(M_{H^\pm} - M_H, M_{H^\pm} - M_A)$ plane (right) planes in 2HDM type-I. The color code indicates the shift from the SM prediction for M_W.
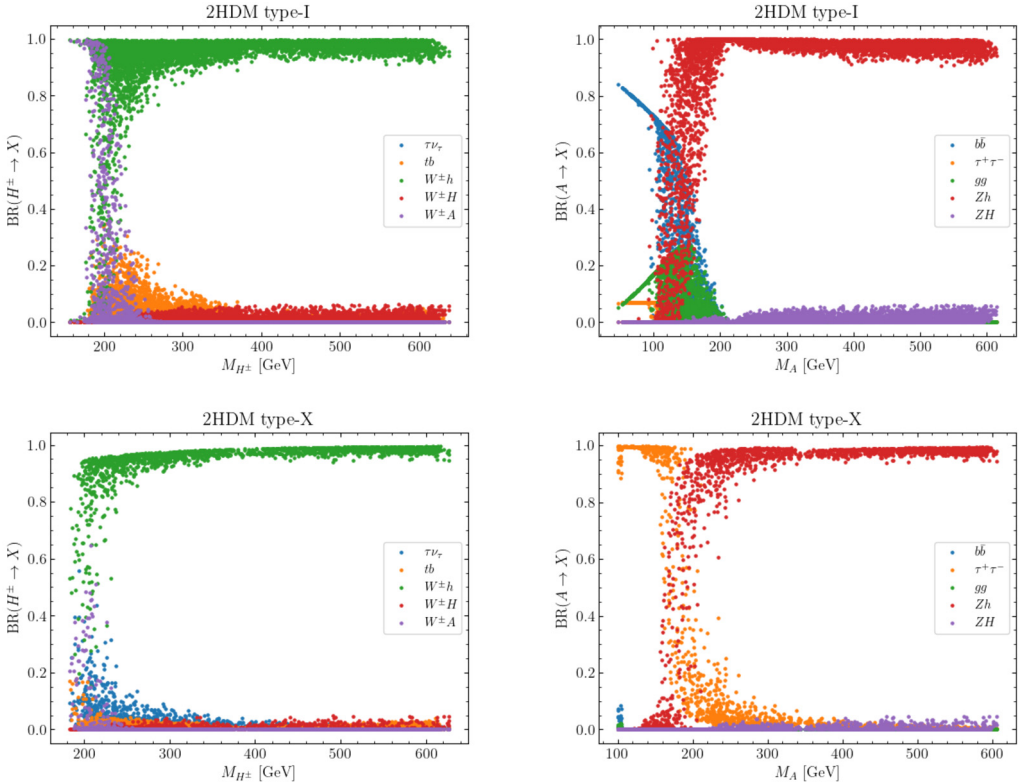

Fig. 3. Branching ratios of the charged Higgs boson as a function of $M_{H^\pm}$ (left) and CP-odd Higgs boson as a function of M_A (right). The upper panels are for 2HDM type-I, while the lower panels are for 2HDM type-X.

decays of the charged Higgs boson are the bosonic channels: $H^\pm \to W^\pm h$ and $H^\pm \to W^\pm A$. For charged Higgs mass less than 200 GeV, both channels $H^\pm \to W^\pm h$ and $H^\pm \to W^\pm A$ compete. The decay $H^\pm \to W^\pm h$ enjoys more phase space because $M_h < 125$ GeV, while the decay

$H^{\pm} \to W^{\pm}A$ is open only for a small portion of the phase space when $M_{H^{\pm}} - M_A > 80$ GeV. In fact, when $H^{\pm} \to W^{\pm}A$ is open it compete strongly with $H^{\pm} \to W^{\pm}h$ because the coupling $H^{\pm}W^{\mp}A$ is a pure gauge coupling while $H^{\pm}W^{\mp}h$ is suppressed by $\cos(\beta - \alpha)$. This is why we can see that, in some cases, the channel $H^{\pm} \to W^{\pm}A$ is the dominant one. The channel $H^{\pm} \to W^{\pm}H$ is negligible since it is suppressed by the parameter $\sin(\beta - \alpha)$ which is small in our scenario. Note that in 2HDM type-I, charged Higgs coupling to fermions is proportional to $1/\tan\beta$, which makes $H^{\pm} \to tb, \tau\nu$ channels rather suppressed. We stress here that the dominance of the bosonic channels has been discussed previously in [64–68].

In Fig. 3 (upper-right panel), we depict the branching ratios of A as a function of M_A. It is visible that before the Zh threshold, the pseudo-scalar boson A decays dominantly into a pair of bottom quarks followed by $A \to gg$ and $A \to \tau\tau$ decays. The loop decay $A \to \gamma\gamma$ is suppressed by $1/\tan^2\beta$ and is smaller than 10^{-3}. Once we cross the Zh threshold, the decay channel $A \to Zh$ becomes the dominant one when $M_A > M_Z + M_h$ since the coupling AZh is proportional to $\cos(\beta - \alpha)$ that is close to unity in our scenario. The channel $A \to ZH$ is suppressed by $\sin(\beta - \alpha)$ being close to vanishing. Note that $A \to H^{\pm}W^{\mp}$ mode is kinematically not open after taking into account the CDF M_W measurement since $M_A < M_{H^{\pm}}$. This is, indeed, a strong effect of this new CDF measurement that closes the possibility to probe the charged Higgs boson via $A \to H^{\pm}W^{\mp}$ and/or $H \to H^{\pm}W^{\mp}$ decay channels.

Note that in the case of 2HDM type-X, as illustrated in Fig. 3 (lower panels), we found that the charged Higgs decay dominantly to $W^{\pm}h$ once the $W^{\pm}h$ threshold is crossed. Before the $W^{\pm}h$ threshold, there is a strong competition between $\tau\nu$, W^+h and W^+A channels, see Fig. 3 (lower-left panel). Similarly, for the decay of the CP-odd Higgs, before the opening of $A \to Zh$, the channel $A \to \tau\tau$ is the dominant one and gets suppressed once $A \to Zh$ is open, see Fig. 3 (lower-right panel).

Before we end this section, we illustrate in Fig. 4 (upper-left and lower-left panels) the correlation between $R_{\gamma\gamma}(H) = \mathrm{BR}(H \to \gamma\gamma)/\mathrm{BR}(H \to \gamma\gamma)_{\mathrm{SM}}$ and $R_{\gamma Z}(H) = \mathrm{BR}(H \to \gamma Z)/\mathrm{BR}(H \to \gamma Z)_{\mathrm{SM}}$ for the SM-like Higgs both in 2HDM type-I and type-X. It is clear that $R_{\gamma Z}(H)$ is all time in the range $[0.85, 1]$ while $R_{\gamma\gamma}(H) \in [0.77, 0.97]$. One can see that they are linearly correlated with $R_{\gamma Z}(H)$ slightly larger than $R_{\gamma\gamma}(H)$ both in 2HDM type-I and type-X. However, in 2HDM type-X, the ranges of $R_{\gamma\gamma}(H)$ and $R_{\gamma Z}(H)$ are a bit smaller compared to 2HDM type-I. In Fig. 4 (upper-right panel), we illustrate the branching ratios of the light CP-even h in 2HDM type-I. One can read that before the WW^* threshold, the dominant decay of h is into a pair of bottoms followed by $h \to \gamma\gamma$ which could reach values above 90% close to the fermiophobic limit. In 2HDM type-X, as illustrated in Fig. 4 (lower-right panel), the decay $h \to \tau\tau$ is the dominant decay channel with a branching ratio almost above 99%. One can also read that $\mathrm{BR}(h \to b\bar{b})$ does not exceed 10% and $\mathrm{BR}(h \to \mu^+\mu^-)$ becomes of the order 3×10^{-3}. It is also clear from Fig. 4 that, in 2HDM type-I, one can have the CP-even h as light as 15 GeV while in 2HDM type-X we have $m_h > 63$ GeV.

4. Conclusion

Recently, CDF released its new measurement for the W boson mass with unprecedented accuracy. The new CDF measurement presents a deviation from the SM prediction with a significance of 7σ. We have shown that in 2HDM in the inverted hierarchy, it is possible to solve the tension between the new CDF M_W measurement and the SM prediction. We found that to comply with the CDF measurement, we need a positive T, and this is only possible in the case where $M_{H^{\pm}} > M_h, M_H, M_A$. The case $M_{H^{\pm}} < M_h, M_H, M_A$ fails to reproduce the correct M_W mea-
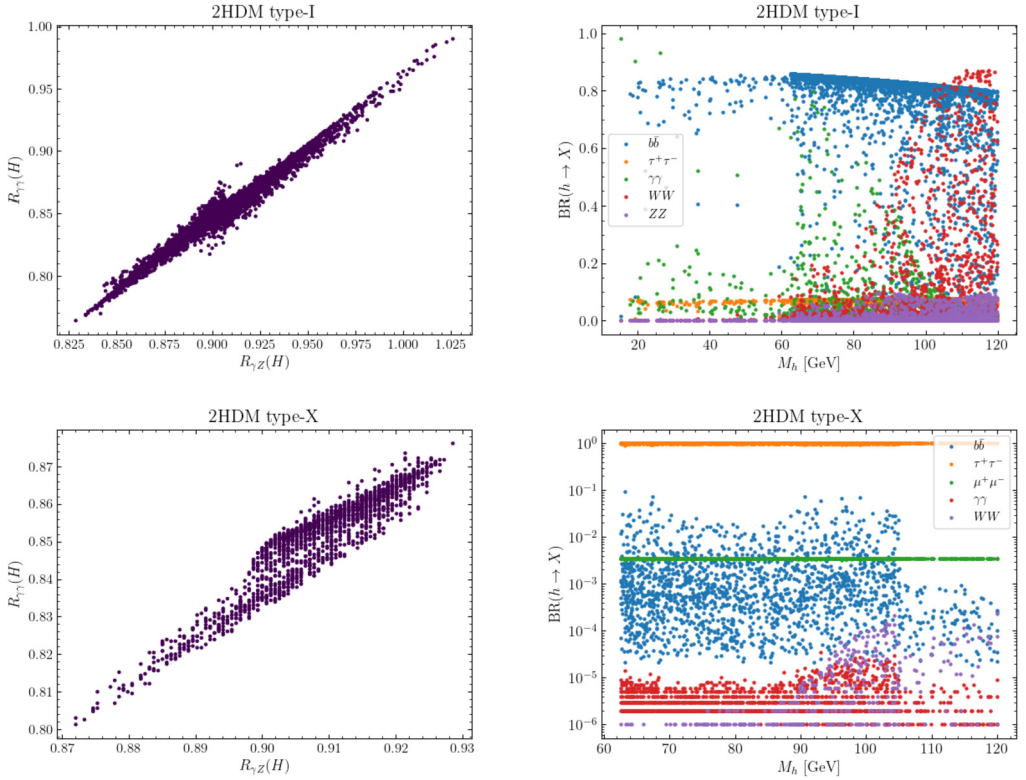
Fig. 4. Left: Correlation between $R_{\gamma\gamma}(H)$ and $R_{\gamma Z}(H)$ for the SM-like Higgs. Right: Branching ratios for the light CP even Higgs boson. The plots are for 2HDM type-I (upper panels) and type-X (lower panels).

surement. We have noticed that the new CDF measurement for M_W pushes the charged Higgs to be larger than about 155 GeV. We also found that the degenerate case $M_{H^\pm} = M_A$ which leads to a very small T parameter is being excluded. We have presented a phenomenology of charged Higgs, CP-odd and the light CP-even Higgsses by illustrating their branching ratios in type-I and type-X of 2HDM. In the case of charged Higgs, we have observed that the bosonic decay $H^\pm \to W^\pm h$ is the dominant one in both types of interest. While for the case of CP-odd, we have noticed that $A \to Zh$, once open, is the dominant mode in 2HDM type-I and -X. However, before the Zh threshold, $A \to bb$ is the dominant mode for 2HDM type-I while $A \to \tau\tau$ would dominate in the case of 2HDM type-X. We have also shown that in this scenario and within 2HDM type-X, BR($h \to \mu^+\mu^-$) could be of the order 3×10^{-3}.

Note Added: While we were finishing this work, we received a paper [21] dealing with a similar 2HDM study, both in normal and inverted hierarchies. In the case of inverted hierarchy, our results are in good agreement.

CRediT authorship contribution statement

Equal Contribution by all the authors and the author names are arranged alphabetically.

Declaration of competing interest

The authors declare that they have no known competing financial interests or personal relationships that could have appeared to influence the work reported in this paper.

Data availability

No data was used for the research described in the article.

Acknowledgements

Appendix A. Allowed points by the $\chi^2_{M_W^{\text{CDF}}}$ test
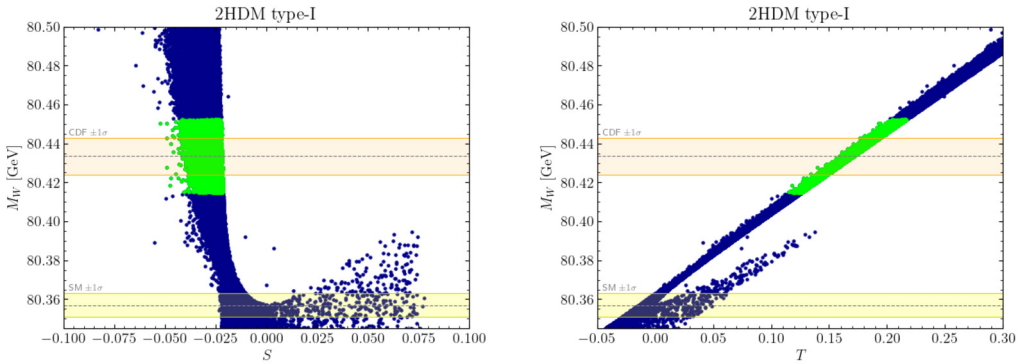
Fig. A.1. The 2HDM prediction for the W boson mass as a function of S (left panel) and T (right panel). The light green band represents points within the CDF 2σ M_W measurement.
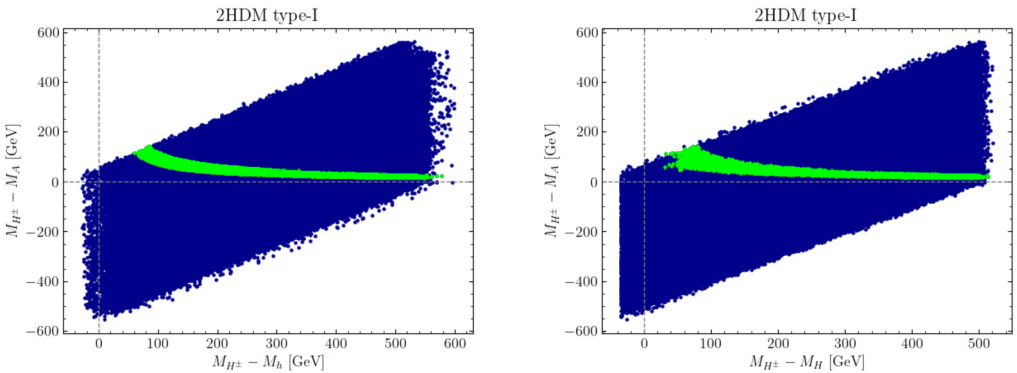

Fig. A.2. Points from the scan in the $(M_{H^\pm} - M_h, M_{H^\pm} - M_A)$ plane (left panel) and $(M_{H^\pm} - M_H, M_{H^\pm} - M_A)$ plane (right panel). The light green band represents points within the CDF 2σ M_W measurement.

Appendix B. PDG and CDF comparison

For the purpose of comparison with the above analysis, we applied here the χ^2_{ST} test (instead of $\chi^2_{M_W^{CDF}}$) before and after the CDF W boson mass measurement [8], denoted by PDG and CDF, respectively:
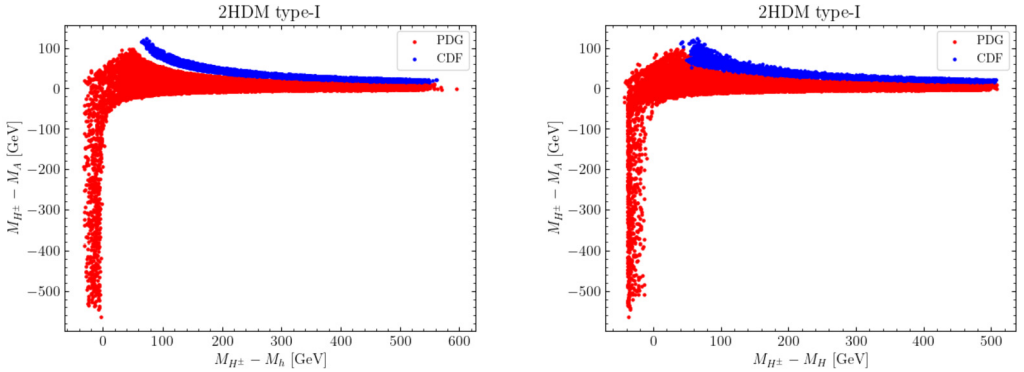

Fig. B.1. Points from the scan in the $(M_{H^\pm} - M_h, M_{H^\pm} - M_A)$ plane (left) and $(M_{H^\pm} - M_H, M_{H^\pm} - M_A)$ plane (right) in 2HDM type-I.
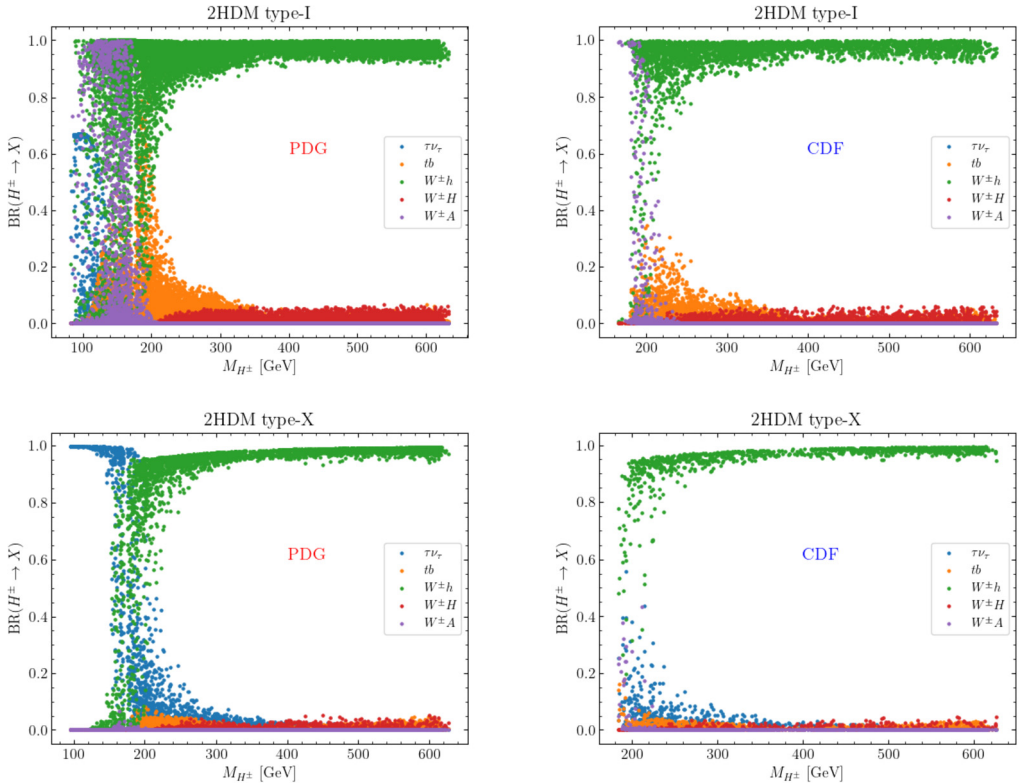

Fig. B.2. Branching ratios of the charged Higgs boson as a function of $M_{H^\pm}$. The left (right) panel represents the PDG (CDF) results. The upper (lower) panels are for 2HDM type-I (type-X).
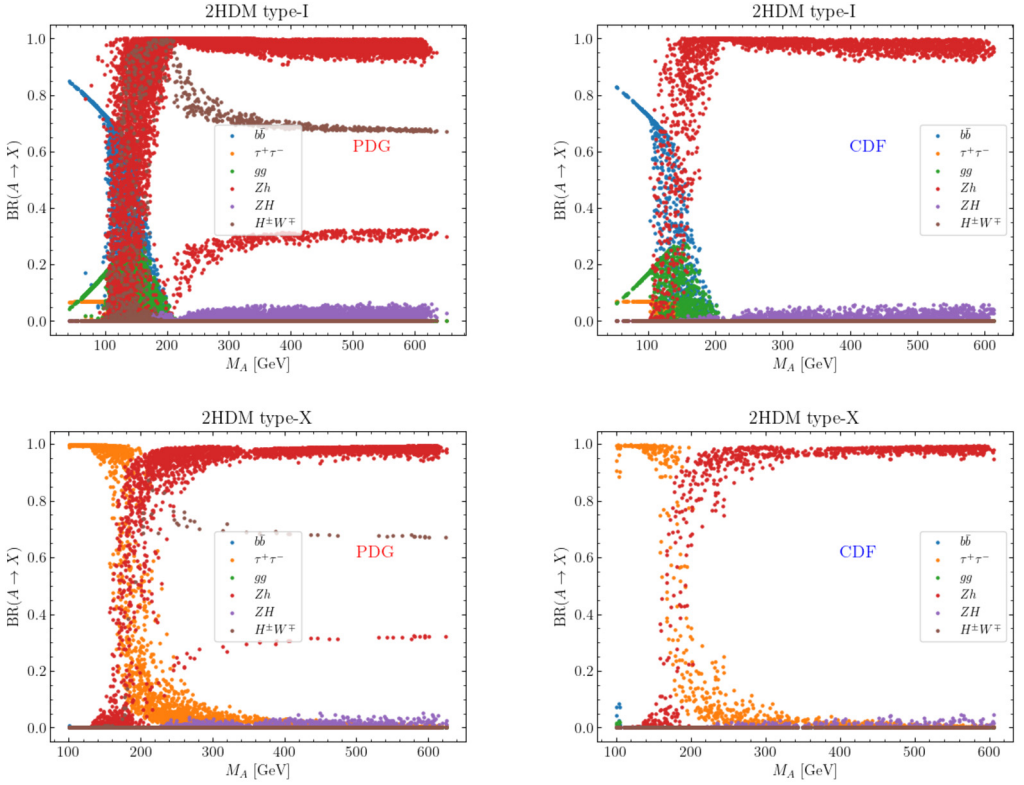
11

Fig. B.3. Branching ratios of the CP-odd Higgs boson as a function of M_A. The left (right) panel represents the PDG (CDF) results. The upper (lower) panels are for 2HDM type-I (type-X).
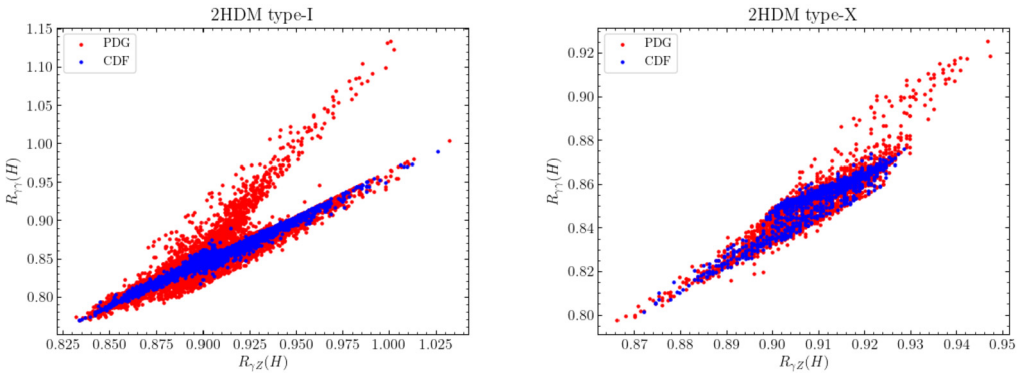

Fig. B.4. Correlation between $R_{\gamma\gamma}(H)$ and $R_{\gamma Z}(H)$ for the SM-like Higgs. The left (right) panel are for 2HDM type-I (type-X).

$$\text{PDG} : S = 0.05 \pm 0.08, \quad T = 0.09 \pm 0.07, \quad \rho_{ST} = 0.92, \tag{B.1}$$

$$\text{CDF} : S = 0.15 \pm 0.08, \quad T = 0.27 \pm 0.06, \quad \rho_{ST} = 0.93, \tag{B.2}$$

where ρ_{ST} is the correlation factor between S and T. We then reproduce similar plots, as shown in Section 3, based on the χ^2_{ST} test. The conclusions remain intact. (See Figs. B.1–B.4.)

References

[1] T. Aaltonen, et al., CDF collaboration, Science 376 (2022) 170–176.

[2] T. Aaltonen, et al., CDF, arXiv:2110.14878 [hep-ex].

[3] P.A. Zyla, et al., Particle Data Group, PTEP 2020 (8) (2020) 083C01.

[4] M. Awramik, M. Czakon, A. Freitas, G. Weiglein, Phys. Rev. D 69 (2004) 053006, arXiv:hep-ph/0311148 [hep-ph].

[5] M.E. Peskin, T. Takeuchi, Phys. Rev. Lett. 65 (1990) 964–967.

[6] M.E. Peskin, T. Takeuchi, Phys. Rev. D 46 (1992) 381–409.

[7] W. Grimus, L. Lavoura, O.M. Ogreid, P. Osland, Nucl. Phys. B 801 (2008) 81–96, arXiv:0802.4353 [hep-ph].

[8] C.T. Lu, L. Wu, Y. Wu, B. Zhu, arXiv:2204.03796 [hep-ph].

[9] A. Broggio, E.J. Chun, M. Passera, K.M. Patel, S.K. Vempati, J. High Energy Phys. 11 (2014) 058, arXiv:1409.3199 [hep-ph].

[10] Y.Z. Fan, T.P. Tang, Y.L.S. Tsai, L. Wu, arXiv:2204.03693 [hep-ph].

[11] H. Song, W. Su, M. Zhang, arXiv:2204.05085 [hep-ph].

[12] H. Bahl, J. Braathen, G. Weiglein, arXiv:2204.05269 [hep-ph].

[13] K.S. Babu, S. Jana, V.P. K, arXiv:2204.05303 [hep-ph].

[14] T. Biekötter, S. Heinemeyer, G. Weiglein, arXiv:2204.05975 [hep-ph].

[15] X.F. Han, F. Wang, L. Wang, J.M. Yang, Y. Zhang, arXiv:2204.06505 [hep-ph].

[16] Y. Heo, D.W. Jung, J.S. Lee, arXiv:2204.05728 [hep-ph].

[17] Y.H. Ahn, S.K. Kang, R. Ramos, arXiv:2204.06485 [hep-ph].

[18] R. Benbrik, M. Boukidi, B. Manaut, arXiv:2204.11755 [hep-ph].

[19] G. Arcadi, A. Djouadi, arXiv:2204.08406 [hep-ph].

[20] K. Ghorbani, P. Ghorbani, arXiv:2204.09001 [hep-ph].

[21] S. Lee, K. Cheung, J. Kim, C.T. Lu, J. Song, arXiv:2204.10338 [hep-ph].

[22] X.K. Du, Z. Li, F. Wang, Y.K. Zhang, arXiv:2204.05760 [hep-ph].

[23] A. Ghoshal, N. Okada, S. Okada, D. Raut, Q. Shafi, A. Thapa, arXiv:2204.07138 [hep-ph].

[24] S. Kanemura, K. Yagyu, arXiv:2204.07511 [hep-ph].

[25] A. Addazi, A. Marciano, A.P. Morais, R. Pasechnik, H. Yang, arXiv:2204.10315 [hep-ph].

[26] J.M. Yang, Y. Zhang, arXiv:2204.04202 [hep-ph].

[27] A. Strumia, arXiv:2204.04191 [hep-ph].

[28] K. Sakurai, F. Takahashi, W. Yin, arXiv:2204.04770 [hep-ph].

[29] X. Liu, S.Y. Guo, B. Zhu, Y. Li, arXiv:2204.04834 [hep-ph].

[30] L. Di Luzio, R. Gröber, P. Paradisi, arXiv:2204.05284 [hep-ph].

[31] P. Asadi, C. Cesarotti, K. Fraser, S. Homiller, A. Parikh, arXiv:2204.05283 [hep-ph].

[32] J.J. Heckman, arXiv:2204.05302 [hep-ph].

[33] E. Bagnaschi, J. Ellis, M. Madigan, K. Mimasu, V. Sanz, T. You, arXiv:2204.05260 [hep-ph].

[34] A. Paul, M. Valli, arXiv:2204.05267 [hep-ph].

[35] R. Balkin, E. Madge, T. Menzo, G. Perez, Y. Soreq, J. Zupan, arXiv:2204.05992 [hep-ph].

[36] M. Endo, S. Mishima, arXiv:2204.05965 [hep-ph].

[37] M.D. Zheng, F.Z. Chen, H.H. Zhang, arXiv:2204.06541 [hep-ph].

[38] L.M. Carpenter, T. Murphy, M.J. Smylie, arXiv:2204.08546 [hep-ph].

[39] O. Popov, R. Srivastava, arXiv:2204.08568 [hep-ph].

[40] T.A. Chowdhury, J. Heeck, S. Saad, A. Thapa, arXiv:2204.08390 [hep-ph].

[41] V. Cirigliano, W. Dekens, J. de Vries, E. Mereghetti, T. Tong, arXiv:2204.08440 [hep-ph].

[42] A. Bhaskar, A.A. Madathil, T. Mandal, S. Mitra, arXiv:2204.09031 [hep-ph].

[43] S. Baek, arXiv:2204.09585 [hep-ph].

[44] J. Cao, L. Meng, L. Shang, S. Wang, B. Yang, arXiv:2204.09477 [hep-ph].

[45] J. Kawamura, S. Okawa, Y. Omura, arXiv:2204.07022 [hep-ph].

[46] K.I. Nagao, T. Nomura, H. Okada, arXiv:2204.07411 [hep-ph].

[47] K.Y. Zhang, W.Z. Feng, arXiv:2204.08067 [hep-ph].

[48] D. Borah, S. Mahapatra, N. Sahu, arXiv:2204.09671 [hep-ph].

[49] Y. Cheng, X.G. He, F. Huang, J. Sun, Z.P. Xing, arXiv:2204.10156 [hep-ph].

[50] A. Batra, S.K. A, S. Mandal, R. Srivastava, arXiv:2204.09376 [hep-ph].

[51] J. de Blas, M. Pierini, L. Reina, L. Silvestrini, arXiv:2204.04204 [hep-ph].

[52] G.C. Branco, P.M. Ferreira, L. Lavoura, M.N. Rebelo, M. Sher, J.P. Silva, Phys. Rep. 516 (2012) 1–102, arXiv:1106.0034 [hep-ph].

[53] S.L. Glashow, S. Weinberg, Phys. Rev. D 15 (1977) 1958.

[54] D. Eriksson, J. Rathsman, O. Stal, Comput. Phys. Commun. 181 (2010) 189–205, arXiv:0902.0851 [hep-ph].

[55] G. Aad, et al., ATLAS CMS, Phys. Rev. Lett. 114 (2015) 191803, arXiv:1503.07589 [hep-ex].

[56] P. Bechtle, D. Dercks, S. Heinemeyer, T. Klingl, T. Stefaniak, G. Weiglein, J. Wittbrodt, Eur. Phys. J. C 80 (12) (2020) 1211, arXiv:2006.06007 [hep-ph].

[57] P. Bechtle, S. Heinemeyer, T. Klingl, T. Stefaniak, G. Weiglein, J. Wittbrodt, Eur. Phys. J. C 81 (2) (2021) 145, arXiv:2012.09197 [hep-ph].

[58] J. Haller, A. Hoecker, R. Kogler, K. Mönig, T. Peiffer, J. Stelzer, Eur. Phys. J. C 78 (8) (2018) 675, arXiv:1803.01853 [hep-ph].

[59] F. Mahmoudi, Comput. Phys. Commun. 180 (2009) 1579–1613, arXiv:0808.3144 [hep-ph].

[60] S. Schael, et al., OPAL, SLD ALEPH, DELPHI, L3, LEP Electroweak Working Group SLD Electroweak Group SLD Heavy Flavour Group, Phys. Rep. 427 (2006) 257–454, arXiv:hep-ex/0509008 [hep-ex].

[61] T. Abe, R. Sato, K. Yagyu, J. High Energy Phys. 07 (2015) 064, arXiv:1504.07059 [hep-ph].

[62] J. Kim, S. Lee, P. Sanyal, J. Song, Phys. Rev. D 106 (3) (2022) 035002, arXiv:2205.01701 [hep-ph].

[63] D. Lopez-Val, J. Sola, Eur. Phys. J. C 73 (2013) 2393, arXiv:1211.0311 [hep-ph].

[64] A. Arhrib, R. Benbrik, S. Moretti, Eur. Phys. J. C 77 (9) (2017) 621, arXiv:1607.02402 [hep-ph].

[65] H. Bahl, T. Stefaniak, J. Wittbrodt, J. High Energy Phys. 06 (2021) 183, arXiv:2103.07484 [hep-ph].

[66] A. Arhrib, R. Benbrik, M. Krab, B. Manaut, S. Moretti, Y. Wang, Q.S. Yan, J. High Energy Phys. 10 (2021) 073, arXiv:2106.13656 [hep-ph].

[67] Y. Wang, A. Arhrib, R. Benbrik, M. Krab, B. Manaut, S. Moretti, Q.S. Yan, J. High Energy Phys. 12 (2021) 021, arXiv:2107.01451 [hep-ph].

[68] A. Arhrib, R. Benbrik, M. Krab, B. Manaut, S. Moretti, Y. Wang, Q.S. Yan, Symmetry 13 (12) (2021) 2319, arXiv:2110.04823 [hep-ph].